

Physics and Modeling of Nano-Transistors

Dr. Yogesh S. Chauhan
 Professor
 Department of Electrical Engineering
 IIT Kanpur, India
 Email: chauhan@iitk.ac.in
 Homepage – <http://home.iitk.ac.in/~chauhan/>

Outline


- Compact Modeling
- Bulk MOSFET and FinFET
- Negative Capacitance FET

07/09/2020 Yogesh Chauhan, IITK 2


My Group and Nanolab

Current members – 35

- Postdoc – 4
- Ph.D. – 19
- Ten PhD graduated



	2020	2019	2018	2017	2016
Books		1			1
Journal	9	14	20	19	18
Conference	8	15	19	11	30



Device Characterization Lab
 - Pulsed IV/RF
 - PNA-X 43.5GHz
 - High Power IV
 - Load Pull

Yogesh Chauhan, IITK

Alumni (PhD) of Nanolab

S. No.	Year	Name	Current Status
10.	2020	Girish Pahwa	Postdoc at UC Berkeley
9.	2020	Shantanu Agnihotri	Asst. Prof. at PEC Chandigarh
8.	2020	Chetan Gupta	Micron Hyderabad
7.	2018	Priyank Rastogi	Intel Bangalore
6.	2018	Prateek Jain	Postdoc at IIT Bombay
5.	2018	Avirup Dasgupta	Postdoc at UC Berkeley
4.	2017	Sheikh Aamir Ahsan	Asst. Prof. at NIT Srinagar
3.	2017	Chandan Yadav	Asst. Prof. at NIT Calicut
2.	2017	Harshit Agarwal	Asst. Prof. at IIT Jodhpur
1.	2017	Pragya Kushwaha	SAC, ISRO

07/09/2020 Yogesh Chauhan, IITK 4

Joint Development & Collaboration



Yogesh Chauhan, IITK

Outline

- Compact Modeling
- Bulk MOSFET and FinFET
- Negative Capacitance FET

07/09/2020 Yogesh Chauhan, IITK 6

Bulk MOSFET

- Drain current in MOSFET (ON operation)

$$I_{ON} = \mu \frac{W}{L} C_{ox} \frac{1}{2} (V_{DD} - V_{TH})^2$$
- Drain current in MOSFET (OFF operation)

$$I_{OFF} \propto 10^{\left(\frac{V_{GS} - V_{TH}}{S}\right)}$$

$C_{ox} = \epsilon_{ox}/t_{ox}$ = oxide cap.
 S = Subthreshold slope
- Desired
 - High I_{ON} ($\downarrow L$, $\uparrow C_{ox}$, $\uparrow V_{DD} - V_{TH}$)
 - Low I_{OFF} ($\uparrow V_{TH}$, $\uparrow S$)

07/09/2020
Yogesh Chaitan, IITK
7

Technology Scaling

- Each time the minimum line width is reduced, we say that a new **technology node** is introduced.
- Example: 90 nm, 65 nm, 45 nm, 32 nm, 22 nm
 - Numbers refer to the minimum metal line width.
 - Poly-Si gate length may be even smaller.

07/09/2020
Yogesh Chaitan, IITK
Figure source - Wikipedia
8

IC industry for >40 years

- Closer distance between elements – **Pitch**
 - Faster** signal transfer and processing rate
- For the same Chip size (or cost), **more functionality**
- Mass production** – Wafer size doubled every 10 years.
- Use less energy (or **power**) for same function
- In the last 45 years since 1965
 - Price** of memory/logic gates has dropped 100 million times.
- The primary engine that powered the proliferation of electronics is **“miniaturization”**.
- More circuits on each wafer → cheaper circuits.
- Miniaturization is key to the improvements in **speed and power consumption** of ICs.

It's not technology! → It's economy.

07/09/2020
Yogesh Chaitan, IITK
9

Technology Trend

07/09/2020
Source: www.intel.com
Yogesh Chaitan, IITK

Wasn't that smooth ride?

- Where is the bottleneck?

$$I_{ON} = \mu \frac{W}{L} C_{ox} \frac{1}{2} (V_{DD} - V_{TH})^2$$

- V_{TH} and Subthreshold Slope can't be decreased

07/09/2020
Yogesh Chaitan, IITK
11

Thin Depletion Layer - Problem

- $Q_G = Q_i + Q_b$
- Charge sharing

07/09/2020
Yogesh Chaitan, IITK
12

Short Channel – Big Problem

Drain Current, I_{ds} (A/ μm)

Gate Voltage, V_{gs} (V)

Smaller size

Gate

Source

Drain

C_d

MOSFET becomes "resistor" at small L.

Chenming Hu, "Modern Semiconductor Devices for ICs" 2010, Pearson

07/09/2020 Yogesh Chaudhan, IITK 13

Making Oxide Thin is Not Enough

Gate

Source

Drain

Leakage Path

Gate cannot control the leakage current paths that are far from the gate.

07/09/2020 Yogesh Chaudhan, IITK 14

What can we do?

Gate

Source

Drain

Leakage Path

07/09/2020 Yogesh Chaudhan, IITK 15

MOSFET in sub-22nm era

FinFET

FDSOI

New Transistor Grows in the Third Dimension

The new 3rd transistor provides higher performance by increasing the conductive area between the source and drain regions of the chip, allowing more current to flow through.

TRADITIONAL TRANSISTOR
Planar conductive area

NEW INTEL TRANSISTOR
Conductive area is expanded on three sides of a raised fin

Source Drain Gate

Silicon substrate

07/09/2020 NY Times

Soitec announces industrial readiness of complete Fully Depleted (FD) platform – Key to higher performance for mobile consumer devices

New platform enables planar FD technology, the only planar solution to sustain Moore's law

From the **Semicon West trade show, San Francisco, July 12, 2010** – The Soitec Group (Euronext Paris), the world's leading supplier of engineered substrates for the microelectronics industry, announced today that the company is ready with the Ultra-Thin Buried Oxide (UTBOX) extension to its Ultra-Fin (UF) silicon-on-insulator (SOI) platform, thereby providing a robust substrate solution for chip designers tackling the performance, power and density challenges of mobile consumer devices. Fully Depleted (FD) planar body transistors are now recognized as the right path on the CMOS roadmap for the 22nm generation and beyond. With FD planar transistor technology on UTBOX wafers, chip designers can enhance their usual design flow and techniques. High-volume capacity is available for the 22nm node at Soitec's manufacturing sites in France and Singapore.

"Soitec is ready with the UTBOX wafers for planar FD architectures: the infrastructure, the process maturity, yield and the capacity are all in place to support demand," said Soitec president and chairman, André-Jacques Auberton-Hervé. "Industry leaders confirm that FD planar technology is the right choice for mobile consumer products, which need higher performance without compromising power. Our UTBOX offering shows the critical role our materials play as the starting point for energy-efficient, state-of-the-art electronics."

07/09/2020 SOITEC

One Way to Eliminate Si Far from Gate

Thin body controlled By multiple gates.

Gate

Source

Drain

Gate

FinFET body is a thin Fin.

Gate Length

Source

Drain

Fin Height

Fin Width

N. Lindert et al., DRC paper II.A.6, 2001

07/09/2020 intel, IBM, tsmc Yogesh Chaudhan, IITK 17

40nm FinFET – 1999

30nm Fin allows 2.7nm SiO₂ & undoped body riding random dopant fluctuation.

Drain current I_d (A/ μm)

Gate voltage V_g [V]

$V_d = 0.05 \text{ V}, 1.05 \text{ V}$

66mV/dec

Measured

Simulated

07/09/2020 X. Huang et al., IEDM, p. 67, 1999 Yogesh Chaudhan, IITK 18

Introduced New Scaling Rule

Leakage is well suppressed if
Fin thickness < L_g

10nm L_g AMD 2002 IEDM	5nm L_g TSMC 2004 VLSI	3nm L_g KAIST 2006 VLSI
--	--	---

07/09/2020 Yogesh Chaudhan, IITK 19

State-of-the-Art **14nm** FinFET

Transistor Fin Improvement

Taller and Thinner Fins for increased drive current and performance

07/09/2020 Source: Anandtech 20

2nd Way to Eliminate Si far from Gate

Ultra-thin-body SOI (UTB-SOI)

Y.K. Choi, IEEE EDL, p. 254, 2000

07/09/2020 Yogesh Chaudhan, IITK 21

Another MOSFET architecture – Gate-All-Around or Surround Gate

[Samsung, VLSI 2009]

DRAM Cell Transistor – 4F² layout

07/09/2020 22

Outline

- Compact Modeling
- Bulk MOSFET and FinFET
- Negative Capacitance FET

07/09/2020 Yogesh Chaudhan, IITK 23

BSIM-CMG and BSIM-IMG

- Berkeley **Short-channel IGFET Model**
- **First industry standard** SPICE model for IC simulation
- Used by hundreds of companies for IC design since 1997
- **BSIM FinFET model** became industry standard in March 2012

It's Free

07/09/2020 Yogesh Chaudhan, IITK 24

BSIM-CMG: Industry standard FinFET model

- Selected as Industry standard 2012

FinFETs on Bulk and SOI Substrates

Vertical CG FET, Horizontal Nanowire FET, Twin Silicon Nanowire FET

07/09/2020 Yogesh Chaudhan, IITK 25

BSIM-CMG Core Models

- Four device architectures
 - Double Gate
 - Double Gate / Trigate / FinFET
 - Quadruple Gate
 - Cylindrical Gate / Nanowire FET
- Three core models
 - Intrinsic Double Gate Core (Y. Taur et al, IEEE EDL, 2004)
 - Perturbation based DG Core for high-doping
 - Cylindrical Gate Core
- Bulk and SOI Substrate

07/09/2020 Yogesh Chaudhan, IITK 26

Short Channel (2D) Effects

- Along the channel - 2D
- Quasi-2D analysis

$$\frac{1}{r} \frac{\partial}{\partial r} \left(\frac{\partial \psi}{\partial r} \right) + \frac{\partial^2 \psi}{\partial y^2} = \frac{qN_A}{\epsilon_{Si}}$$

$$\frac{d^2 \psi_{eff}}{dy^2} + \frac{V_{eff} - V_{fb} - \psi_{eff}}{\lambda^2} = \frac{qN_A}{\epsilon_{Si}}$$

Characteristic Length $\lambda = \sqrt{\frac{R^2}{4} + \frac{\epsilon_{Si}}{2qN_A} R}$

- Similar expression for Double Gate and FinFET/Trigate
- Analytical expressions model
 - Threshold Voltage roll off
 - Drain induced barrier lowering (DIBL)
 - Sub-threshold swing degradation

Symbols: TCAD Results; Lines: Model

07/09/2020 Yogesh Chaudhan, IITK
Auth and Plummer, IEEE EDL, 2007

Quantum Mechanical Effects

- Predictive model for confinement induced V_{th} shift due to band splitting present in the model
- Can choose to use an effective τ_{ox} that accounts for charge centroid behavior with bias
- Effective Width model that accounts for reduction in width for a triple / quadruple / surround gate structure

Width reduction due to structural confinement of inversion charge. (Dotted lines represent the effective width perimeter)

07/09/2020 Yogesh Chaudhan, IITK
S. Venugopalan et al, IEEE TED, 2013

Verification: 30nm to 10 μ m FinFETs

Each curve is for one L_g
Symbols: Data; Lines: BSIM-CMG Model

07/09/2020 Yogesh Chaudhan, IITK

Temperature Model verified for FinFET

07/09/2020 Yogesh Chaudhan, IITK 30

FinFET's Various Complex Cross-Sections

TSMC, IEDM 2010

Leti, VLSI 2012

IBM, VLSI 2012

Toshi VLSI 2012

Yogesh Chaudhan, IITK

Prior Models Available for Two Simple Cross-Sections Only – Deductive model

1. Double-Gate FinFET:

Charge Equation:

$$V_G - V_{FB} + \frac{t_{ox}}{2\epsilon_{ox}} Q_d - V = -\frac{t_{ox}}{2\epsilon_{ox}} Q_c + v_T \ln \frac{Q_c(Q_c + Q_d)}{q_{Si}^2 W_{sil} [1 - \exp \frac{W_{sil}}{4v_T \epsilon_{sil}} (Q_c + Q_d)]}$$

2. Cylindrical FinFET:

Charge Equation:

$$V_G - V_{FB} + \frac{\ln(1+t_{ox}/R)}{2\epsilon_{ox}} Q_d C_{cy} - V = -\frac{\ln(1+t_{ox}/R)}{2\epsilon_{ox}} Q_c C_{cy} + v_T \ln \frac{-Q_c C_{cy} + \sqrt{Q_c^2 C_{cy}^2 + 4q_{Si}^2 R^2}}{2q_{Si}^2 v_T R} + v_T \ln \frac{-Q_c C_{cy} + \sqrt{Q_c^2 C_{cy}^2 + 4q_{Si}^2 R^2}}{1 - \exp \frac{Q_c C_{cy}}{4v_T \epsilon_{sil}}}$$

Yogesh Chaudhan, IITK

New Unified Model for Complex FinFET Cross-Sections – Inductive model

$$v_G - v_O - v_{CH} = -q_m + \ln(-q_m) + \ln\left(\frac{q_i^2}{e^{-q_i} - q_i - 1}\right)$$

$$v_O = v_{FB} - q_{dep} - \ln\left(\frac{2q_m^2 A_{ch}}{v_T C_{ins} W_{ch}}\right)$$

$$q_i = (q_m + q_{dep}) \frac{A_{ch} C_{ins}}{\epsilon_{ch} W_{ch}^2}$$

Model Parameters:

- Fin Area: A_{ch}
- Channel Doping: N_{ch}
- Channel Width: W
- Insulator Cap: C_{ins}

Unified Model for various Fin shapes

Yogesh Chaudhan, IITK

Experimental FinFET Example: I-V

SOI FinFET

SOI FinFET $L_G = 10 \mu m$

SOI FinFET $L_G = 10 \mu m$

SOI FinFET $L_G = 10 \mu m$

SOI FinFET $L_G = 10 \mu m$

*FinFET fabricated by SEMATECH

Yogesh Chaudhan, IITK

3D Model for Short Channel Effects

- SCEs are 3-D effects – Need to solve the 3-D Poisson's equation. $\nabla^2 \psi(x, y, z) = -\frac{qN_{ch}}{\epsilon_{ch}}$
- DIBL Equations: $\Delta V_{TH} = f(\vec{V}, \lambda)$ $SS = g(\vec{V}, \lambda)$
- λ : characteristic field penetration length

$$\lambda_{DG} \approx \frac{\epsilon_{ch} T_{ch} t_{ins}}{\epsilon_{ins}}$$

$$\lambda_{CyG} \approx \frac{2\epsilon_{ch} R^2 \ln\left(1 + \frac{t_{ins}}{R}\right)}{\epsilon_{ins}}$$

Unified λ

$$\lambda \approx \sqrt{\frac{\epsilon_{ch} A_{ch}}{C_{ins}}}$$

Yogesh Chaudhan, IITK

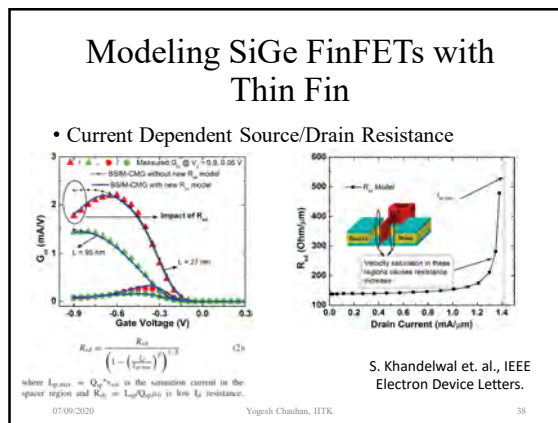
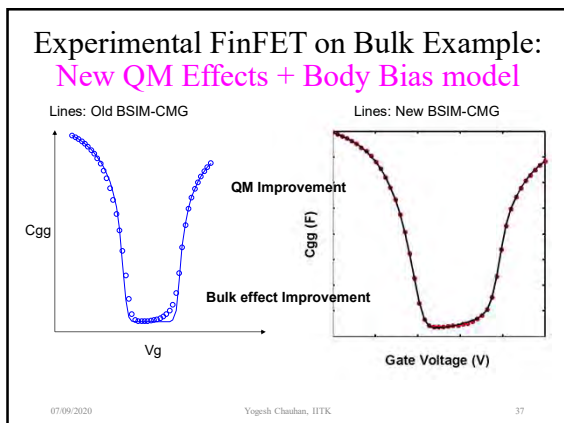
TCAD FinFET Example: I-V: Scaling

Bulk FinFET Lines: Model Symbols: TCAD $V_{ds} = 0.05 V$

Lines: Model Symbols: TCAD

- $H_{sil} = 40nm, EOT = 1nm$
- $T_{fin, top} = T_{fin, bottom} = 15 nm, V_{fb} = 0.9V$
- $T_{fin, top} = T_{fin, bottom} = 15 nm, V_{fb} = 1V$
- $T_{fin, top} = T_{fin, bottom} = 25 nm, V_{fb} = 0.8V$
- $T_{fin, top} = T_{fin, bottom} = 25 nm, V_{fb} = 1V$

Yogesh Chaudhan, IITK



FinFET Modeling for IC Simulation and Design: Using the BSIM-CMG Standard

FinFET Modeling for IC Simulation & Design Using the BSIM-CMG Standard

Yogesh Singh Chauhan
Darsen Lu
Sriramkumar Venugopalan
Sourabh Khandelwal
Juan Pablo Duarte
Navid Paydavosi
Ali Niknejad
Chenming Hu

Chapters

1. FinFET- from Device Concept to Standard Compact Model
2. Analog/RF behavior of FinFET
3. Core Model for FinFETs
4. Channel Current and Real Device Effects
5. Leakage Currents
6. Charge, Capacitance and Non-Quasi-Static Effect
7. Parasitic Resistances and Capacitances
8. Noise
9. Junction Diode Current and Capacitance
10. Benchmark tests for Compact Models
11. BSIM-CMG Model Parameter Extraction
12. Temperature Effects

Available online on Elsevier.

07/09/2020 Yogesh Chauhan, IITK 39

Industry Standard FDSOI Compact Model BSIM-IMG for IC Design

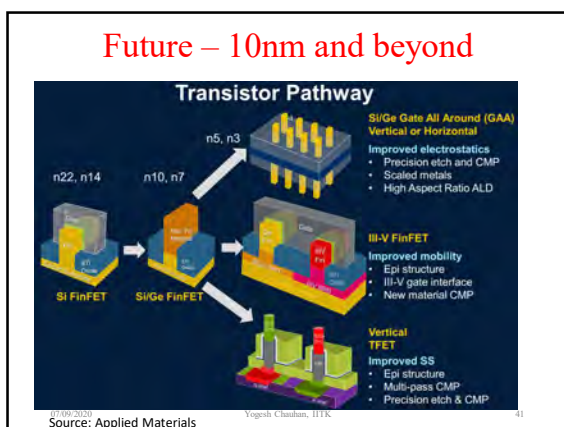
INDUSTRY STANDARD FDSOI COMPACT MODEL BSIM-IMG FOR IC DESIGN

CHENMING HU, SOURABH KHANDELWAL, YOGESH SINGH CHAUHAN, TIGRASEE SIKKOLY, JOSEF WARTS, JUAN PABLO DUARTE, PRAVYA KUSHAWAHA AND HARSHU SACHDEV

Chapters

1. Fully Depleted Silicon on Oxide Transistor and Compact Model
2. Core Model for Independent Multigate MOSFETs
3. Channel Current Model With Real Device Effects in BSIM-IMG
4. Leakage Current and Thermal Effects
5. Model for Terminal Charges and Capacitances in BSIM-IMG
6. Parameter Extraction With BSIM-IMG Compact Model
7. Testing BSIM-IMG Model Quality
8. High-Frequency and Noise Models in BSIM-IMG

07/09/2020 Yogesh Chauhan, IITK 40



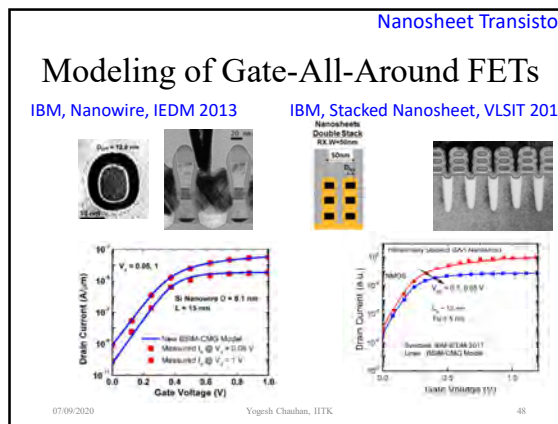
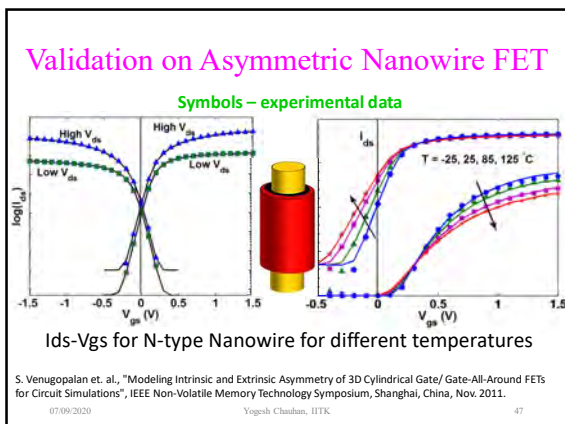
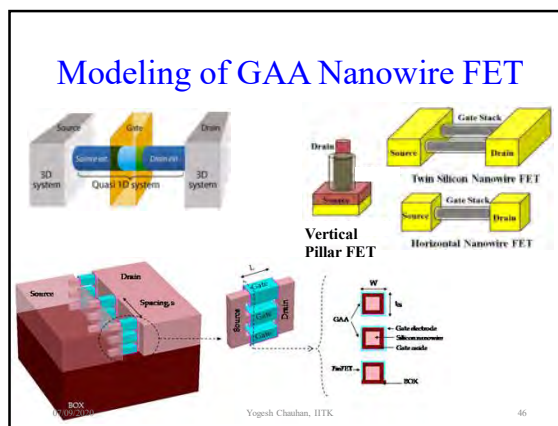
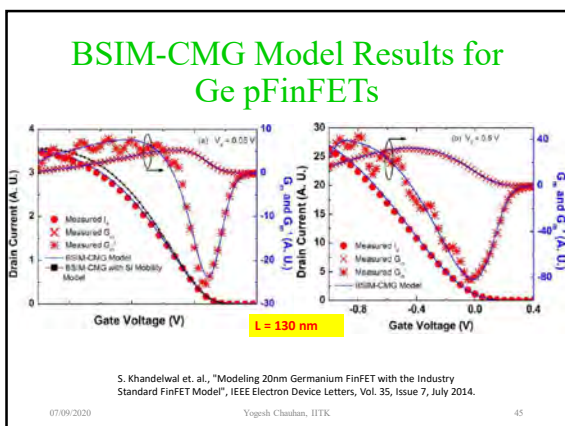
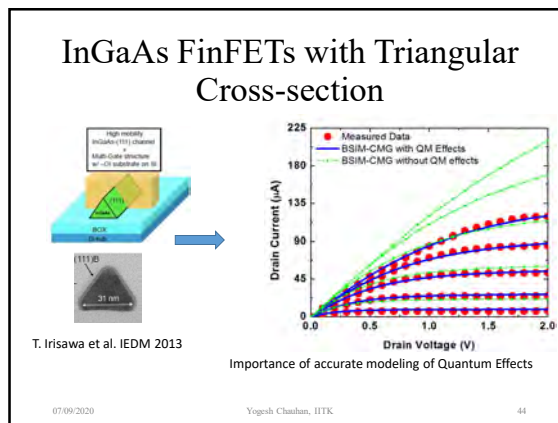
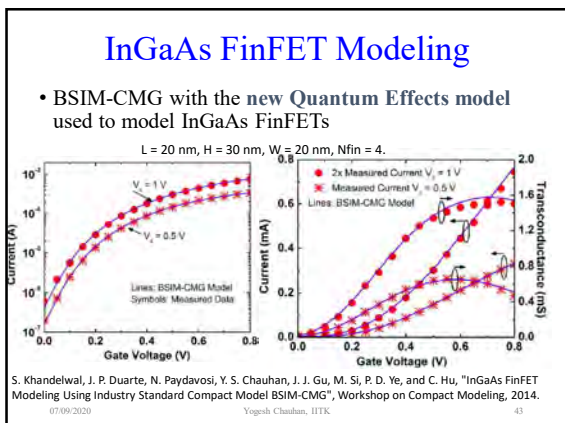
Key points for 10nm and beyond

- Reduced leakage – Better sub-threshold slope
 - Ultra-thin channel
 - Electrostatic control \rightarrow Nanosheet transistors
- Higher mobility channel
 - Si NMOS and PMOS
 - Ge PMOS
 - SiGe
 - III-V materials NMOS – InAs, InGaAs etc.?

$$I_{off}(nA) = 100 \frac{W}{L} 10^{\frac{V_{in}}{S}}$$

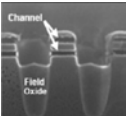
$$I_{dsat} = \frac{W}{2L} C_{ox} \mu_{eff} (V_{gs} - V_t)^2$$

07/09/2020 Yogesh Chauhan, IITK 42

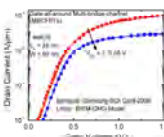


Samsung Multibridge & Twin Nanowire


Samsung, SOI Conf. 2006



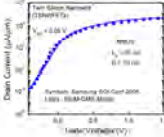
Multi-bridge-channel MOSFET




Samsung, SOI Conf. 2006




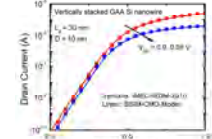
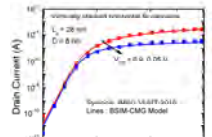
Twin silicon nanowire MOSFET



Stacked GAA Si NW MOSFETs




IMEC, IEDM 2016


TCAD Validation for different cross-sections of GAA Transistors

Ach = 28nm*2, W=18nm, Cins=0.86nF/m




Circular GAA

Ach = 22nm*2, W=18nm, Cins=0.76nF/m

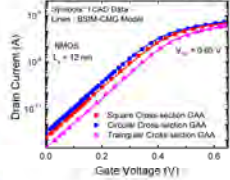


Square GAA

Ach = 14nm*2, W=18nm, Cins=0.73nF/m



Triangular GAA

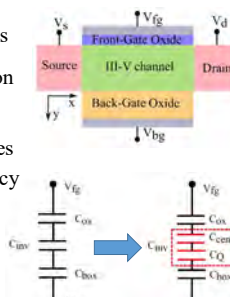


7nm & beyond – Would it be a smooth ride?

- Effects in ultra-thin Si/Ge/III-V Transistors
 - Quantum Capacitance
 - Charge centroid
 - Source to Drain Tunneling
 - Bandgap variation with thickness
 - Effective mass variation with thickness

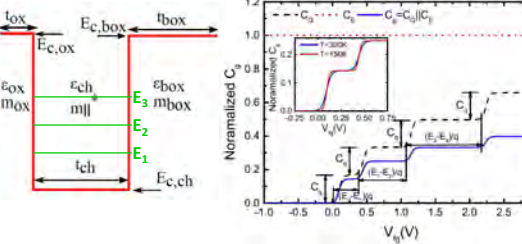
Quantum Capacitance

- Quantum capacitance originates when vertical electric field partially penetrates the inversion charge in channel.
- The quantum capacitance depends on 2-D density of states $\rho_{2D} = \frac{m_{||}}{\pi \hbar^2}$ and valley degeneracy factor (g_v)
- Quantum Capacitance $C_Q = \frac{q^2 g_v m_{||}^*}{\pi \hbar^2}$



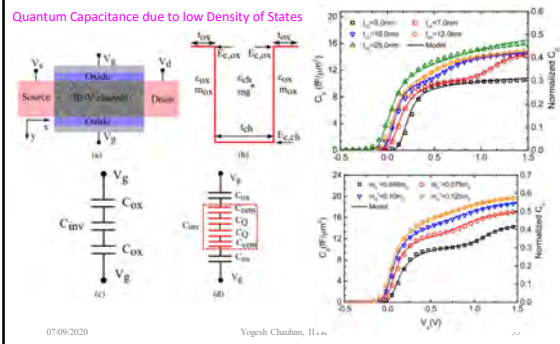
Quantum Capacitance

Thin body device is a 2D system.



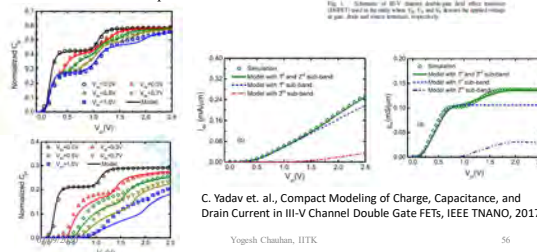
C. Yadav et. al., submitted in Solid State Electronics.

Quantum Capacitance in III-V FinFETs



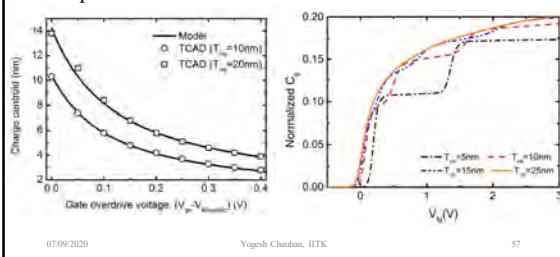
Modeling of III-V Channel DG-FETs

- Conduction band nonparabolicity
- 2-D density of states
- Quantum capacitance in low DOS materials
- Contribution of multiple subbands



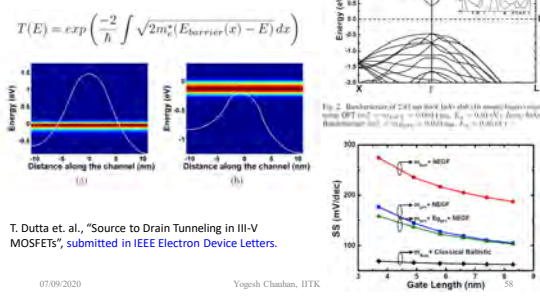
Charge centroid

- Charge centroid in conjunction with Quantum capacitance can deteriorate C-V further.

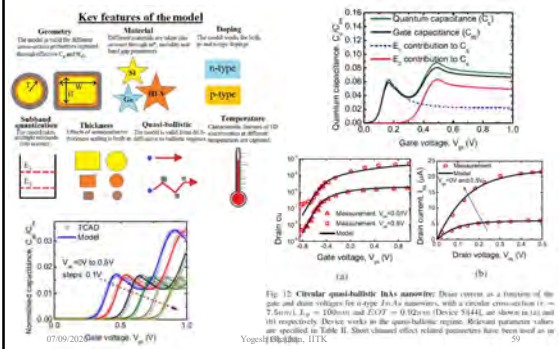


Source to Drain Tunneling in III-V FETs

- Under the barrier transport

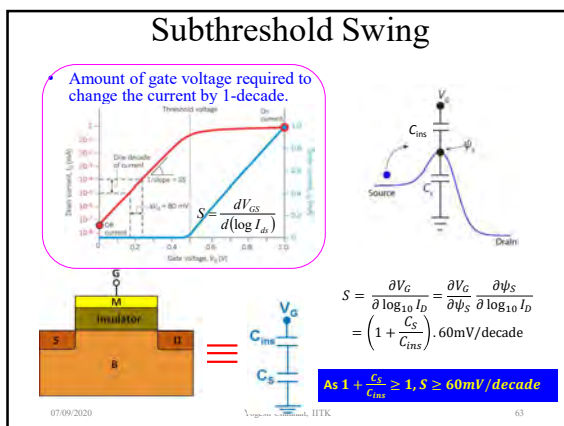
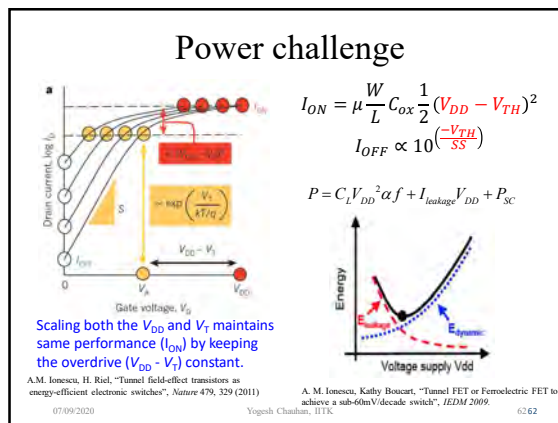
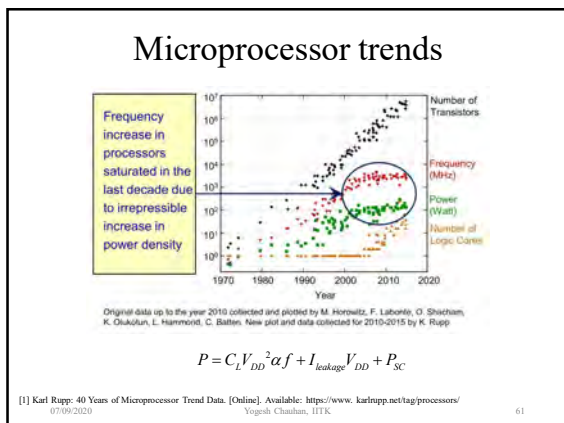


Modeling of Quasi-ballistic Nanowire FETs



Outline

- Compact Modeling
- Bulk MOSFET and FinFET
- Negative Capacitance FET

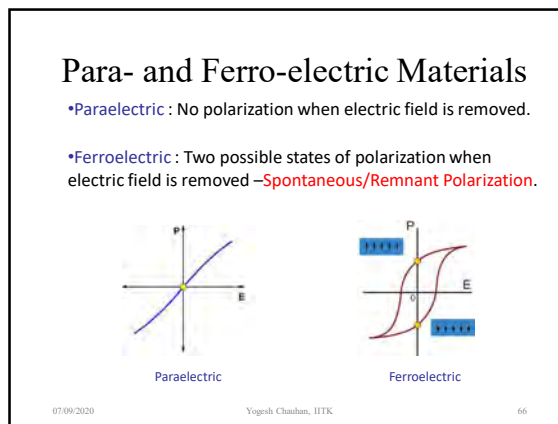
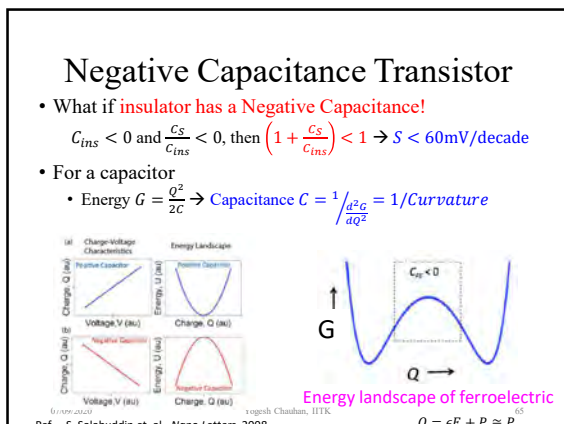


Capacitance Definition

- In general, insulator can be a **non-linear dielectric** whose **capacitance density (per unit volume)** can be defined as
 - 1: $C_{ins} = \left(\frac{\partial^2 G}{\partial P^2}\right)^{-1}$ = inverse curvature of free energy density
 - 2: $C_{ins} = \frac{\partial P}{\partial E}$ = slope of the polarization vs electric field curve

P = Polarization in dielectric, G = Free energy density, E = Externally applied electric field

- Two types of non-linear dielectrics:
 - Paraelectric : No polarization when electric field is removed.
 - Ferroelectric : Two possible states of polarization when electric field is removed.



Ferroelectricity

Requirements:

- Spontaneous electric polarization: Non-Centrosymmetric (for crystalline materials)
- Reversible polarization state by the application of electric field

e.g. Lead titanate PbTiO₃, HZO

Centrosymmetric:- Paraelectric

Pb²⁺, O²⁻, Ti⁴⁺

P=0 at E=0

Non-Centrosymmetric:- Ferroelectric

Classical Ferroelectric PbTiO₃ (Pb²⁺Ti⁴⁺O₆)

E=0

a=0.3905 nm

c=0.412 nm

δ=pm

P ≠ 0 at E=0

[1] K. M. Rabe, C. H. Ahn, and J.-M. Triscone, Eds., *Physics of Ferroelectrics: A Modern Perspective*, vol. 105, Berlin, Germany: Springer, 2007.
[2] A.I. Khalilov, *Negative Capacitance for Ultra-low Power Computing*, PhD thesis, University of California at Berkeley, 2015.

Paraelectric to Ferroelectric Phase Transition

e.g. Pb(Zr_{1-x}Ti_x)O₃ Lead Zirconium Titanate (PZT)

Paraelectric phase

T > T_C

Cubic

Ferroelectric phase

T < T_C

Tetragonal

T_C = Curie Temperature

07/09/2020 Yegesh Chaudhan, IITK 68

[1] K. M. Rabe, C. H. Ahn, and J.-M. Triscone, Eds., *Physics of Ferroelectrics: A Modern Perspective*, vol. 105, Berlin, Germany: Springer, 2007.

Landau-Khalatnikov Theory of Non-Linear Dielectrics

- Free energy of a non-linear dielectric is given as $G = \alpha P^2 + \beta P^4 + \gamma P^6 - EP$
- α and β can be +ve or -ve but γ is always +ve for stability reasons.
- Dynamics of G is given by $\delta \frac{dP}{dt} = -\frac{\partial G}{\partial P}$ δ = Polarization damping factor
- In the steady state, $\frac{dP}{dt} = 0 \Rightarrow E = 2\alpha P + 4\beta P^3 + 6\gamma P^5$

For $\alpha > 0$ and at $E = 0$, there exit only one real root

$P = 0$

A Paraelectric Material

For $\alpha < 0$ and at $E = 0$, there exit three real roots

$P = 0, \pm P_r$ where $P_r = \sqrt{\frac{\sqrt{\beta^2 - 3\alpha\gamma} - \beta}{3\gamma}}$

A Ferroelectric Material has a non-zero P at zero E.

07/09/2020 Yegesh Chaudhan, IITK 69

Assumptions

Free energy of a non-linear dielectric $G = \alpha P^2 + \beta P^4 + \gamma P^6 - EP$

- Polarization and Electric field are uniaxial. (perpendicular to electrodes)
- Polarization and Electric field magnitudes are uniform throughout the ferroelectric.
- Piezo-electricity is ignored.

07/09/2020 Yegesh Chaudhan, IITK 70

L-K explanation of Phase Transition

For $E = 0$, $G = \alpha P^2 + \beta P^4 + \gamma P^6$ and $\alpha = \alpha_0(T - T_0)$, $\alpha_0 > 0$

Paraelectric Material

$E=0$, G , $\alpha > 0$

$0 = 2\alpha P + 4\beta P^3 + 6\gamma P^5$

- $\alpha > 0$ i.e. for $T > T_0$; at $E = 0$, there exists only one real root, $P = 0$
- i.e. No polarization when electric field is removed

$[P = 0 \text{ at } E = 0]$

Ferroelectric Material

$E=0$, G , $\alpha < 0$

- Note, $P = 0$ has a maximum.
- Not possible in an isolated ferroelectric.

$0 = 2\alpha P + 4\beta P^3 + 6\gamma P^5$

- $\alpha < 0$ i.e. for $T < T_0$; at $E = 0$, there exist three real roots $P = 0, \pm P_r$ where $P_r = \sqrt{\frac{\sqrt{\beta^2 - 3\alpha\gamma} - \beta}{3\gamma}}$
- Two possible states of polarization when electric field is removed.

[1] K. M. Rabe, C. H. Ahn, and J.-M. Triscone, Eds., *Physics of Ferroelectrics: A Modern Perspective*, vol. 105, Berlin, Germany: Springer, 2007.

Positive and Negative Capacitances

Paraelectric

A Positive Capacitor

Ferroelectric

A Conditionally Negative Capacitor

Three possible solutions at $E = 0$

$P = 0$ is not possible in a isolated Ferroelectric due to maxima of energy or a negative capacitance

$C_{ins} = \left(\frac{\partial^2 G}{\partial P^2}\right)^{-1} = \frac{\partial P}{\partial E} < 0$

07/09/2020 Yegesh Chaudhan, IITK 72

Application of Electric Field

$G = \alpha P^2 + \beta P^4 + \gamma P^6 - EP$
 $E = 2\alpha P + 4\beta P^3 + 6\gamma P^5$

Paraelectric
 [A Positive Capacitor]

Isolated Ferroelectric
 [A Conditionally Negative Capacitor]

[1] K. M. Rabe, C. H. Ahn, and J.-M. Triscone, Eds., *Physics of Ferroelectrics: A Modern Perspective*, vol. 105, Berlin, Germany: Springer, 2007.
 [2] A.I. Khalil, "Negative Capacitance for Ultra-low Power Computing," PhD thesis, University of California at Berkeley, 2015.

How to stabilize a Negative Capacitance?

Add a positive dielectric capacitance in series such that total free energy of system has a minima in the negative capacitance regime of ferroelectric.

Total energy of the FE + DE system
 $G = G_f + G_d$
 $Q = \epsilon_0 E_f + P_f = \epsilon_0 E_d + P_d$

Assuming V is small
 $Q \approx P_f \approx P_d$

For a stable system $\frac{\partial^2 G}{\partial Q^2} > 0$ (minimum)

$\Rightarrow \frac{1}{C_{tot}} = \frac{1}{C_f} + \frac{1}{C_d} > 0$

For a stable system
 $|C_f| > C_d$

$\Rightarrow \frac{\partial^2 G}{\partial Q^2} = \frac{\partial^2 G_f}{\partial Q^2} + \frac{\partial^2 G_d}{\partial Q^2}$

$C_{tot} = \frac{C_d \cdot |C_f|}{|C_f| - C_d} > 0$

For a stable system
 $C_{tot} > C_d$

Negative Capacitance in Ferroelectric

$C_{ins} = C_{fe}$

Negative slope region can be stabilized if

$C_{total} = \left(\frac{1}{-|C_{fe}|} + \frac{1}{C_s} \right)^{-1} > 0$

or,
 $|C_{fe}| > C_s$

S. Salahuddin and S. Datta, "Use of negative capacitance to provide voltage amplification for low power nanoscale devices," *Nano Letters*, vol. 8, no. 2, pp. 405-410, 2008.

How to stabilize a Negative Capacitance?

- Add a positive dielectric capacitance in series such that total free energy of system has a minima in the negative capacitance regime of ferroelectric.

A. I. Khan et al., *APL*, vol. 99, no. 11, p. 113501, 2011

$\frac{1}{C_{tot}} = \frac{1}{C_{FE}} + \frac{1}{C_{DE}} > 0$

$C_{DE} < |C_{FE}|$ and $C_{FE} < 0$

$C_{tot} = \frac{C_{DE} \cdot |C_{FE}|}{|C_{FE}| - C_{DE}} > 0$

Ferroelectric-Dielectric Systems

A. I. Khan et al., *APL*, vol. 99, no. 11, p. 113501, 2011.

D. J. Appleby et al., *Nano Letters*, vol. 14, no. 7, pp. 3864-3868, 2014.

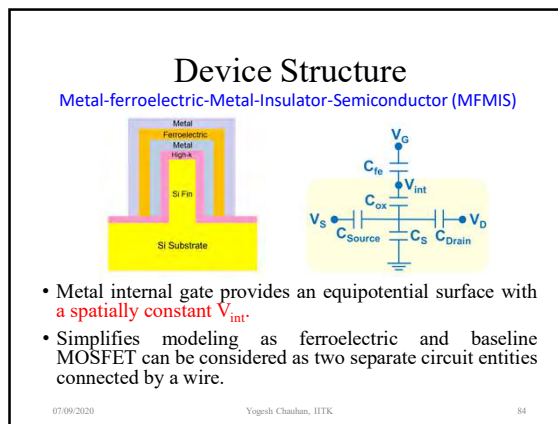
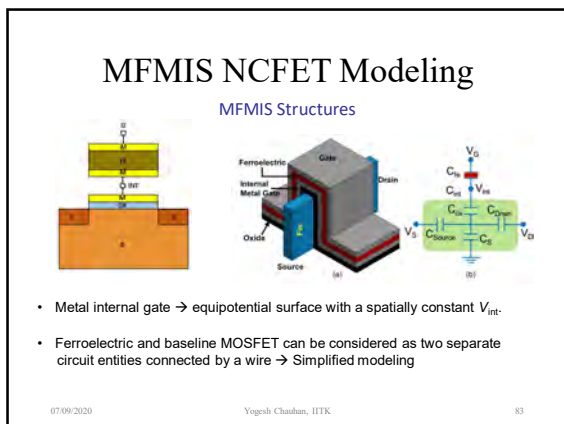
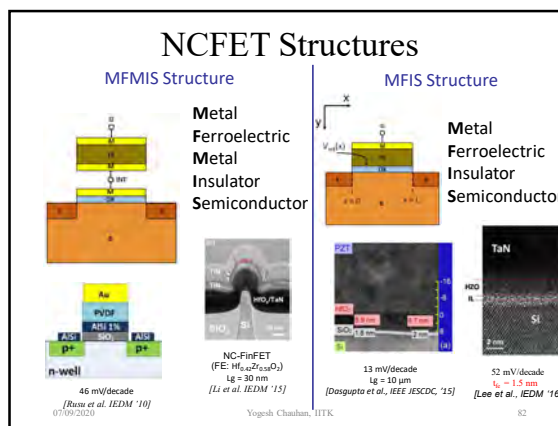
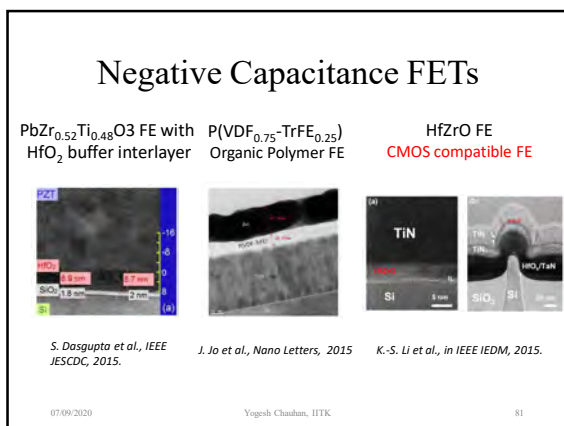
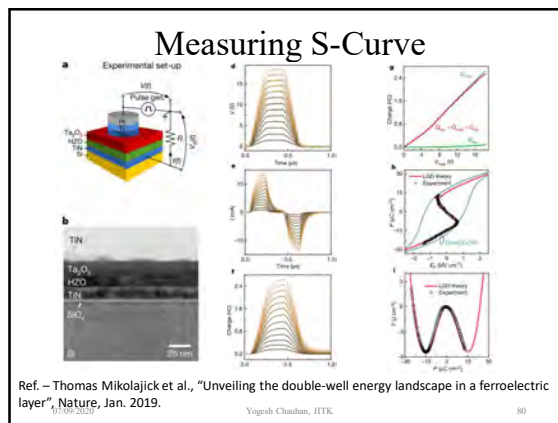
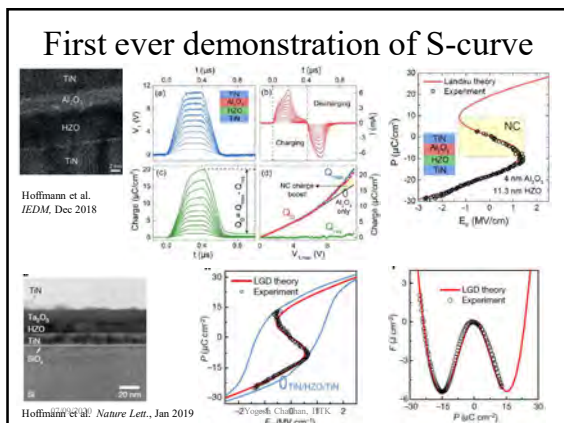
Total Capacitance of Ferroelectric-dielectric hetro-structure becomes greater than the dielectric capacitance.

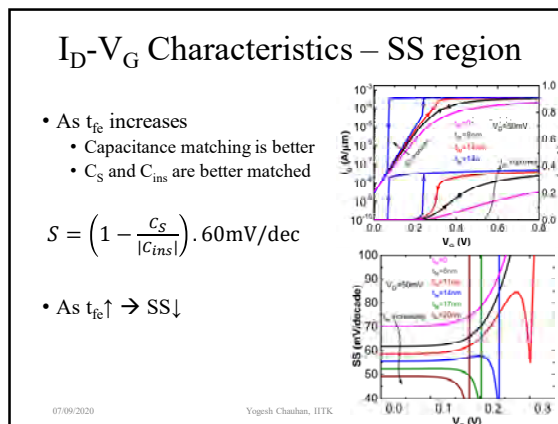
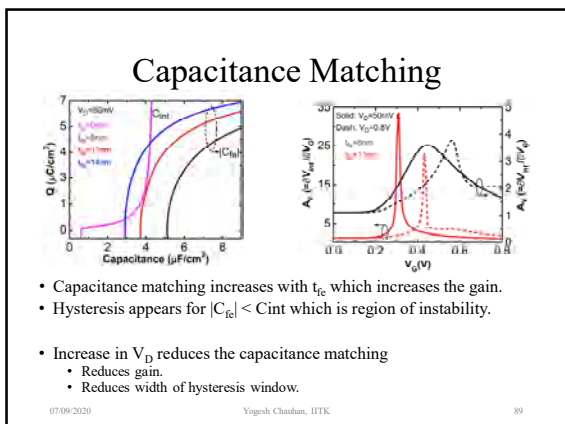
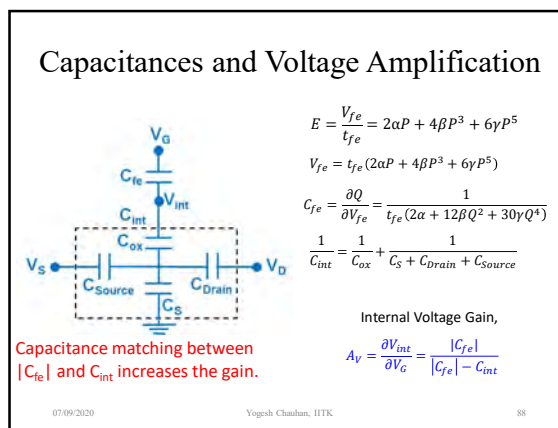
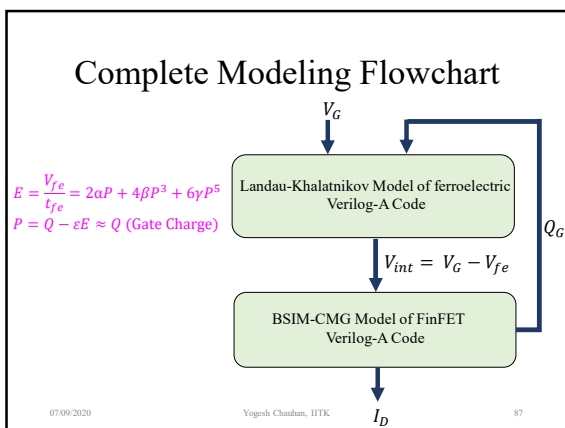
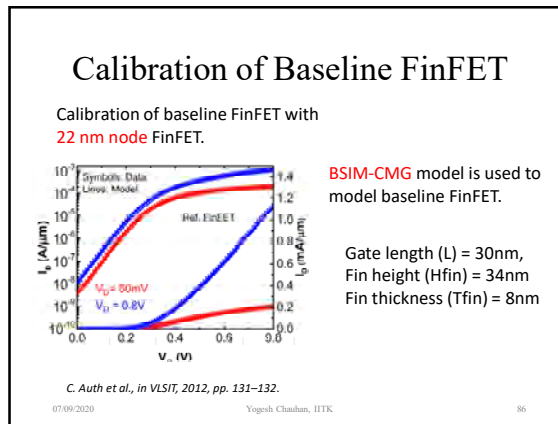
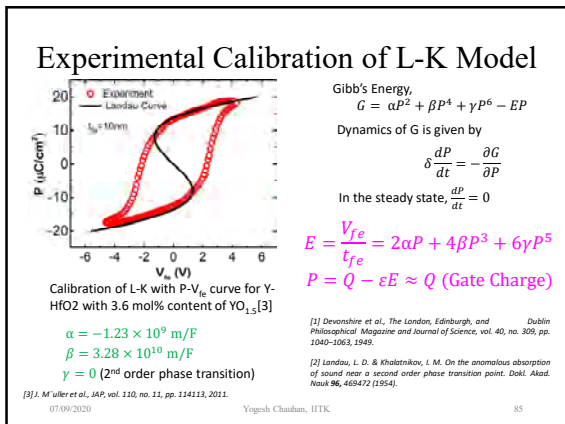
$C_{tot} = \frac{C_{DE} \cdot |C_{FE}|}{|C_{FE}| - C_{DE}} > 0$

Ferroelectric-Resistor System

A. I. Khan et al., "Negative capacitance in a ferroelectric capacitor," *Nature Mater.*, vol. 14, no. 2, pp. 182-186, 2015.

- NC is observed only for a small duration (~μs) during polarization switching.
- Difficult to stabilize.





I_D-V_G Characteristics – ON region

- As t_{fe} increases
 - Capacitance matching is better

$$A_V = \frac{\partial V_{int}}{\partial V_G} = \frac{|C_{fe}|}{|C_{fe}| - C_{int}}$$

- As gain increases, I_{ON} increases.

Note the significant improvement in I_{ON} compared to SS.

07/09/2020 Yogesh Chauhan, IITK 91

I_D-V_G Experimental Demonstration

07/09/2020 Yogesh Chauhan, IITK 92

I_D-V_D Characteristics

- NCFET is biased in negative capacitance region.
 - Q_G or P is positive → V_{fc} is negative.
- V_{DS} ↑ → Q_G or P ↓ → |V_{fc}| ↓ → V_{int} = V_G + |V_{fc}| ↓ → A_V ↓ → Current reduces

G. Pahwa, ..., Y. S. Chauhan, "Analysis and Compact Modeling of Negative Capacitance Transistor with High ON-Current and Negative Output Differential Resistance", IEEE TED, Dec. 2016.

07/09/2020 Yogesh Chauhan, IITK 93

Experimental Demonstration

07/09/2020 Yogesh Chauhan, IITK 94

Negative DIBL

- V_D reduces Q_G which, in turn reduces V_{int} = V_G - V_{fe} in the negative capacitance region.
 - Negative DIBL increases with t_{fe} due to increased V_{fc} drop.
- V_{th} increases with V_D instead of decreasing.
 - Higher I_{ON} still lower I_{OFF}!
 - Higher I_{ON} still lower I_{OFF}!

07/09/2020 Yogesh Chauhan, IITK 95

Negative DIBL/DIBR Effect

- V_D ↑, Q_G ↓, V_{fe} ↑, V_{int} ↓, V_{th} ↑
- V_{th} increases with V_D instead of decreasing. Higher I_{ON} still lower I_{OFF}!
- Negative DIBL increases with t_{fe} due to increased V_{fc} drop.

07/09/2020 Yogesh Chauhan, IITK 96

I_D-V_G Characteristics – High V_{DS}

- Hysteresis appears for $|C_{fe}| < C_{int}$ which is the **region of instability**.
- As t_{fc} increases
 - SS reduces, I_{ON} increases.
 - I_{OFF} reduces for high V_D.
- Width of hysteresis at larger thicknesses can be controlled with V_D.

07/09/2020 Yogesh Chauthan, IITK 97

Negative Output Differential Resistance

G. Pahwa et al., IEEE TED, Dec. 2016
Mengwei Si et al., Nature Nanotechnology, 2016
J. Zhou et al., IEEE, JEDS, 2018
J. Zhou et al., IEDM 2016

07/09/2020 Yogesh Chauthan, IITK 98

Optimum NC-FinFET

- Same I_{ON} as 22 nm node FinFET.
- Steeper SS of 58.2 mV/decade.
- V_{DD} reduction by 0.4 V.
- I_{OFF} reduction by 83 %.

07/09/2020 Yogesh Chauthan, IITK 99

Ferroelectric Parameters Variation

If $\gamma = 0$,

$$\alpha = -\frac{3\sqrt{3}E_c}{P_r} \quad \beta = \frac{3\sqrt{3}E_c}{P_r^3}$$

P_r = Remnant Polarization
 E_c = Coercive Field
 $C_{fe} = \frac{1}{t_{fe}(2\alpha + 12\beta Q^2)}$

- Low P_r and high E_c
 - reduce $|C_{fe}|$ which leads to improved capacitance matching and hence, a high gain.
 - Low SS
 - increase I_{ON} but reduce I_{OFF} due to a more negative DIBL \Rightarrow high I_{ON}/I_{OFF}.

07/09/2020 Yogesh Chauthan, IITK 100
D. Ricinschi et al., JPCM, vol. 10, no. 2, p. 477, 1998.

Intrinsic Delay

Delay, $\tau = \frac{\Delta Q_C}{I_{ON}}$

$$\Delta Q_C = Q_C(V_G = V_D = V_{DD}) - Q_C(V_G = 0, V_D = V_{DD})$$

- NC-FinFET driving NC-FinFET
 - For high V_{DD}, high I_{ON} advantage is limited by large amount of ΔQ_C to be driven.
 - Outperforms FinFET at low V_{DD}.
 - Minimum at V_{DD} \approx 0.28 V corresponds to a sharp transition in Q_C.
- NC-FinFET driving FinFET load provides full advantage of NC-FinFET.

07/09/2020 Yogesh Chauthan, IITK 101

Power and Energy Delay Products

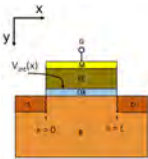
$$PDP = \Delta Q_C \cdot V_{DD}$$

$$EDP = \frac{(\Delta Q_C)^2 V_{DD}}{I_{ON}}$$

- NC-FinFET driving NC-FinFET shows advantage only for low V_{DD}.
- NC-FinFET driving FinFET load is the optimum choice.

07/09/2020 Yogesh Chauthan, IITK 102

Modeling of MFIS NCFET



\$V_{int}(x)\$

Contrast with MFIS structure:

- \$P\$ and \$V_{int}\$ vary spatially in longitudinal direction
- Better stability w.r.t. Leaky ferroelectric and domain formation

Issues with Existing Models^[1,2]:
 Implicit equations – tedious iterative numerical solutions

[1] H.-P. Chen, V. C. Lee, A. Okota, J. Xiang, and Y. Taur, "Modeling and design of ferroelectric MOSFETs," *IEEE Trans. Electron Devices*, vol. 58, no. 8, pp. 2401–2405, Aug. 2011.

[2] D. Jimenez, E. Miranda, and A. Godoy, "Analytic model for the surface potential and drain current in negative capacitance field-effect transistors," *IEEE Trans. Electron Devices*, vol. 57, no. 10, pp. 2405–2409, Oct. 2010.

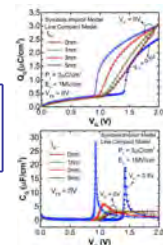
Explicit Modeling of Charge

$V_{fe} = \epsilon \tilde{\eta}_e = a Q_G + b Q_G^3$

Voltage Balance:
 $V_G - V_{FB} = V_{fe} + \frac{Q_G}{C_{ox}} + \psi_S = a_{eff} Q_G + b Q_G^3 + \psi_S$

\$Q_G - \psi_S\$ relation^[1]
 $Q_G = \text{sign}(\psi_S) \gamma C_{ox} \left[\psi_S + V_T (e^{-\psi_S/V_T} - 1) + e^{-(2\phi_F + V_c)/V_T} (V_T e^{\psi_S/V_T} - \psi_S - V_T) \right]^{1/2}$

→ Implicit equation in \$Q_G\$
 → Goal: Explicit Model with good initial guesses for each region of NCFET operation

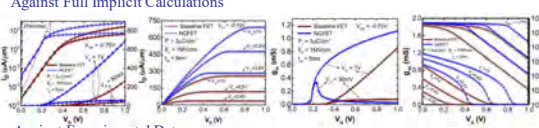


Both the \$Q_G\$ and its derivatives match well with implicit model

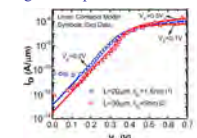
G. Pahwa, T. Dutta, A. Agarwal and Y. S. Chauhan, "Compact Model for Ferroelectric Negative Capacitance Transistor With MFIS Structure," in *IEEE Transactions on Electron Devices*, March 2017.

Drain Current Model Validation

Against Full Implicit Calculations



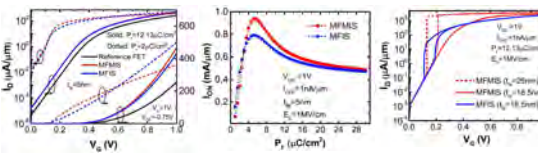
Against Experimental Data



G. Pahwa, T. Dutta, A. Agarwal and Y. S. Chauhan, "Compact Model for Ferroelectric Negative Capacitance Transistor With MFIS Structure," *IEEE Transactions on Electron Devices*, March 2017.

[1] M. H. Lee et al., in *IEDM Tech. Dig.*, Dec. 2016, pp. 12.1.1–12.1.4. [2] M. H. Lee et al., in *IEDM Tech. Dig.*, Dec. 2015, pp. 22.5.1–22.5.4.

MFIS Vs MFMIS



- MFIS excels MFMIS for low \$P_f\$ ferroelectrics only.
- A smooth hysteresis behavior in MFIS compared to MFMIS.
- MFIS is more prone to hysteresis → exhibits hysteresis at lower thicknesses compared to MFMIS.

G. Pahwa, T. Dutta, A. Agarwal, and Y. S. Chauhan, "Physical Insights on Negative Capacitance Transistors in Non-Hysteresis and Hysteresis Regimes: MFMIS vs MFIS Structures", accepted in *IEEE Transactions on Electron Devices*, 2018.

Compact Modeling of MFIS GAA-NCFET

$V_{fe} = a_0 Q + b_0 Q^3$

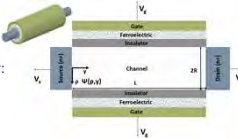
Radial Dependence in Ferroelectric Parameter:
 (Ignored in others work)
 $a_0 = 2\alpha R \ln[1 + t_{fe}/(R + t_{ins})]$
 $b_0 = 2bR^2[1/(R + t_{ins})^2 - 1/(R + t_{ins} + t_{fe})^2]$

Mobile Charge Density:
 $Q = \text{inv} \left(\frac{d\psi}{dx} \right) \Big|_{x=0} = \left(\frac{2\alpha}{R} \right) \left(\frac{2\beta^2}{1-\beta^2} \right)$

Voltage Balance:
 $V_G - \Delta\phi - \psi_S = (a_0 + 1/C_{ox})Q + b_0 Q^3$

Implicit Equation in \$\beta\$:
 $\ln(\beta) - \ln(1 - \beta^2) + m \left(\frac{\beta^2}{1 - \beta^2} \right) + n \left(\frac{\beta^2}{1 - \beta^2} \right)^3 - G = 0$

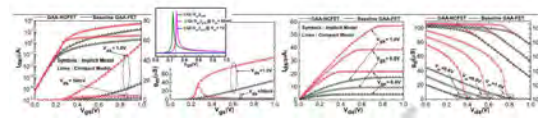
→ Goal: Explicit Model for \$\beta\$ with good initial guess valid in all region of NCFET operation which will be used for further calculation of drain current and terminal charges.



A. D. Gaidhane, G. Pahwa, A. Verma, and Y. S. Chauhan, "Compact Modeling of Drain Current, Charges and Capacitances in Long Channel Gate-All-Around Negative Capacitance MFIS Transistor", accepted in *IEEE Transactions on Electron Devices*, 2018.

Drain Current Model Validation

Against Full Implicit Calculations



- In contrast to bulk-NCFETs
- Multi-gate NCFETs with an undoped body exhibit same \$I_{OFF}\$ and \$V_{th}\$ due to absence of bulk charges.
- GAA-NCFET characteristics show different bias dependence due to the absence of bulk charge.

A. D. Gaidhane, G. Pahwa, A. Verma, and Y. S. Chauhan, "Compact Modeling of Drain Current, Charges and Capacitances in Long Channel Gate-All-Around Negative Capacitance MFIS Transistor", accepted in *IEEE Transactions on Electron Devices*, 2018.

Terminal Charges in GAA-NCFET

- Peak in the gate capacitance is observed where the best capacitance matching occurs between the internal FET and the ferroelectric layer.
- For high V_{DS} , the Q_G for GAA-NCFET saturates to $(4/5)^{th}$ of the maximum value (at $V_{ds} = 0$) in contrast to conventional devices for which it saturates to $(2/3)^{rd}$ of the maximum value.

07/09/2020 Yogesh Chauhan, IITK 109

MFMIS vs MFIS

G. Pahwa, T. Dutta, A. Agarwal, and Y. S. Chauhan, "Physical Insights on Negative Capacitance Transistors in Non-Hysteresis and Hysteresis Regimes: MFMS vs MFIS Structures", IEEE Transactions on Electron Devices, Vol. 65, Issue 3, Mar. 2018.

07/09/2020 Yogesh Chauhan, IITK 110

Comparing I_D-V_G and I_D-V_D Characteristics (long channel)

- MFIS excels MFMS for low P_r ferroelectrics only, in long channel NCFETs.

07/09/2020 Yogesh Chauhan, IITK 111

Understanding different trends with P_r

- Total current in ON regime \approx drift current = inversion charge * horizontal electric field
- For high P_r , charge is higher for MFIS, but electric field in channel is low due to a decreasing V_{int} profile from source to drain, which results in lower current than MFMS.
- For low P_r , charge is lower for MFIS, but electric field in channel is high due to a increasing V_{int} profile from source to drain, which results in higher current than MFMS.

G. Pahwa, T. Dutta, A. Agarwal, and Y. S. Chauhan, "Physical Insights on Negative Capacitance Transistors in Non-Hysteresis and Hysteresis Regimes: MFMS vs MFIS Structures", IEEE Transactions on Electron Devices, Vol. 65, Issue 3, Mar. 2018.

07/09/2020 Yogesh Chauhan, IITK 112

Hysteresis Behavior

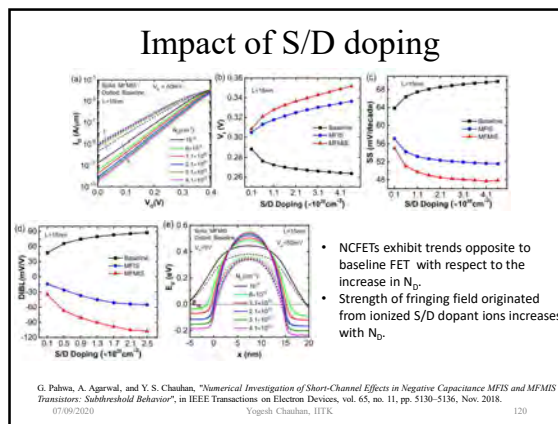
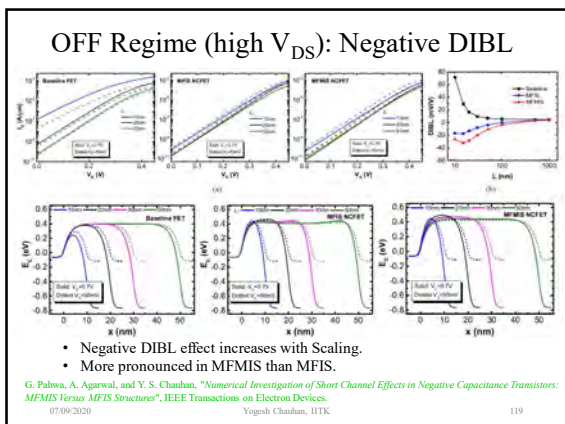
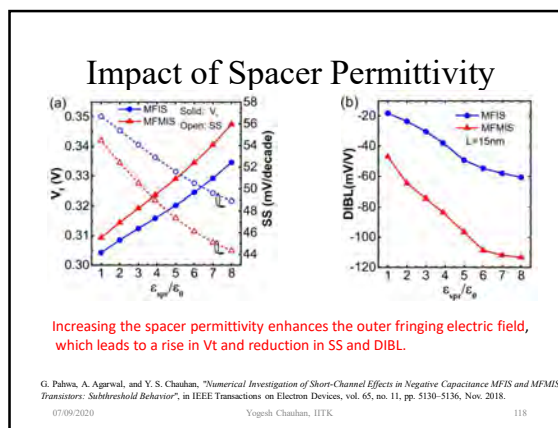
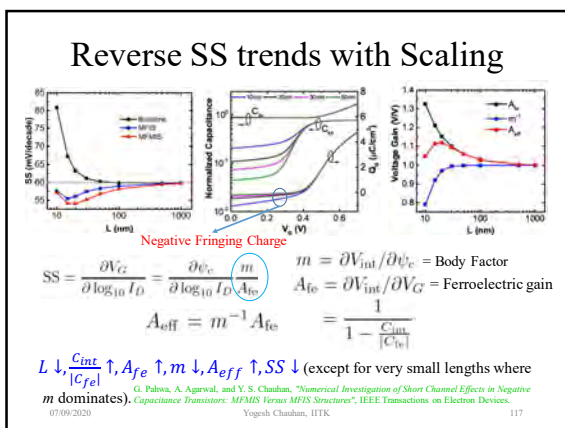
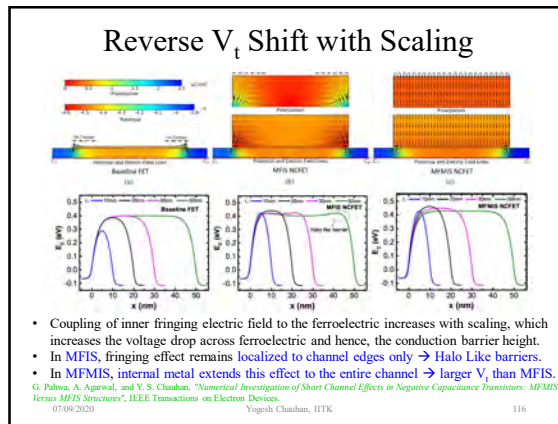
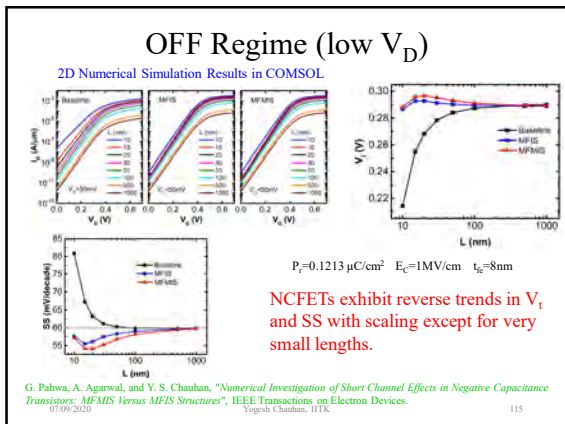
- Continuous switching of dipoles from source to drain results in a **smooth hysteresis behavior in MFIS compared to MFMS** where dipoles behave in unison.
- Source end dipole switches, first, owing to its least hysteresis threshold.
- Non-zero drain bias disturbs capacitance matching in MFMS resulting in a delayed onset of hysteresis.
- MFIS is more prone to hysteresis \rightarrow exhibits hysteresis at lower thicknesses compared to MFMS.

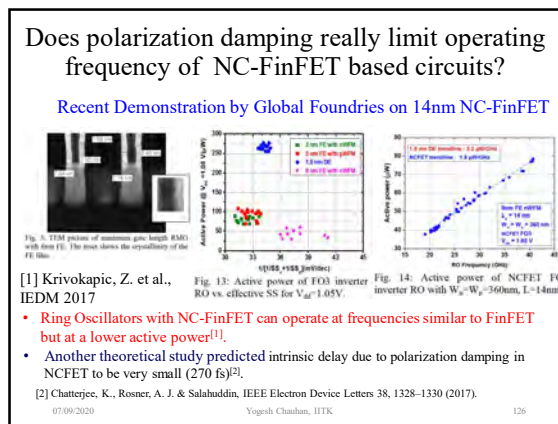
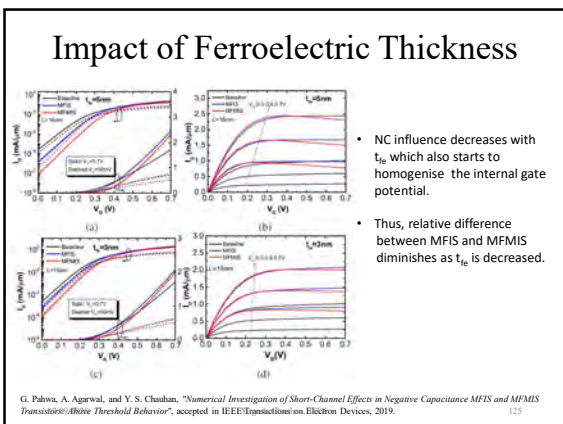
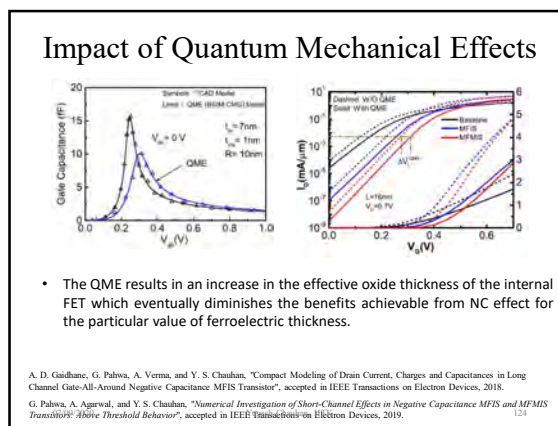
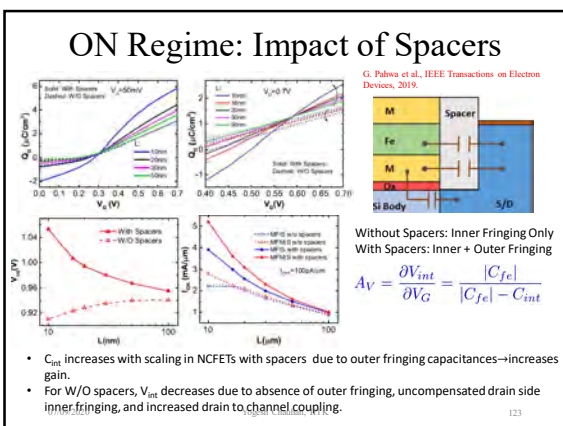
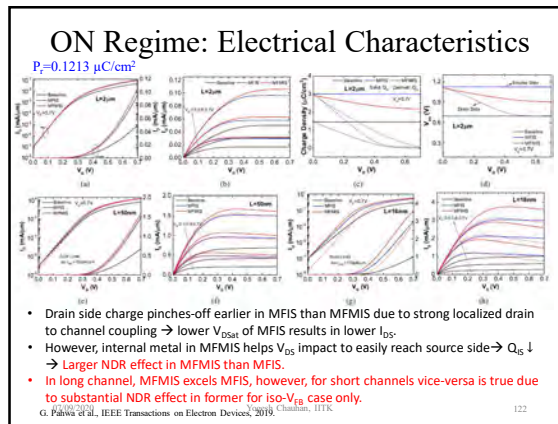
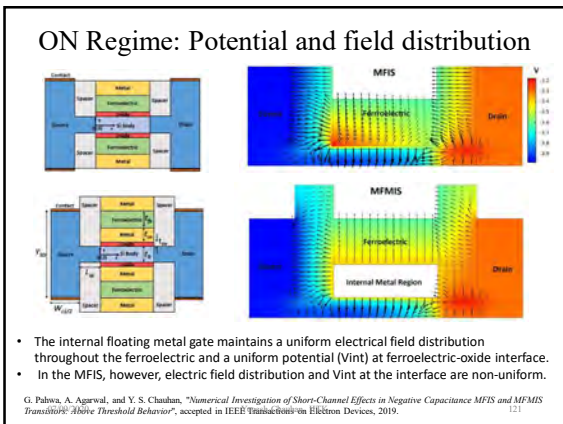
G. Pahwa, T. Dutta, A. Agarwal, and Y. S. Chauhan, "Physical Insights on Negative Capacitance Transistors in Non-Hysteresis and Hysteresis Regimes: MFMS vs MFIS Structures", IEEE Transactions on Electron Devices, Vol. 65, Issue 3, Mar. 2018.

07/09/2020 Yogesh Chauhan, IITK 113

MFMS vs MFIS: Short Channel Effects

07/09/2020 Yogesh Chauhan, IITK 114





NC-FinFET based inverters

• Although the transistor characteristics show no Hysteresis, the VTCs of NC-FinFET inverters can still exhibit it due to the **NDR region in the output characteristics**.

T. Dutta, G. Pahwa, A. R. Trivedi, S. Sinha, A. Agarwal, and Y. S. Chauhan, "Performance Evaluation of 7 nm Node Negative Capacitance FinFET based SRAM", IEEE Electron Device Letters, Aug. 2017.

NC-FinFET based SRAM

- Read time: reduced due to the increased drive current
- Write time: slower due to the gate capacitance enhancement
- P_{avg} : NC-SRAM performs better with lower standby leakage only at small t_{fc} , taking advantage of the lower subthreshold currents

T. Dutta, G. Pahwa, A. R. Trivedi, S. Sinha, A. Agarwal, and Y. S. Chauhan, "Performance Evaluation of 7 nm Node Negative Capacitance FinFET based SRAM", IEEE Electron Device Letters, Aug. 2017.

Effects of NCFET on standard cells: 7nm FinFET standard cell library

- Increasing t_{fc} – larger A_g in transistors (i.e., steeper slope and higher ON current) → Delay of cells become smaller.

07/09/2020 Yogesh Chauhan, IITK IEEE Access 129

Effects of NCFET on standard cells: 7nm FinFET standard cell library

Using a ferroelectric with 1nm, 2nm, 3nm and 4nm thickness provides a speedup of around 15%, 30%, 40% and 45% respectively, in the delay of gates at the operating voltage of 0.7V.

- Quantifying the relative delay decrease/improvement of cells within the 7nm FinFET standard cell library due to NCFET at $V_{DD} = 0.7V$.

07/09/2020 Yogesh Chauhan, IITK 130

Effects of NCFET on standard cells: 7nm FinFET standard cell library

- Increase in t_{fc} leads to an increase in the total cells' capacitance which further increases internal power of the cells.
- Same baseline performance (i.e., frequency) can be achieved at a lower voltage, which leads to quadratic saving in dynamic power and exponential saving in stand-by power, thus, compensating the side effect of NCFET with respect to power.

07/09/2020 Yogesh Chauhan, IITK 131

Effects of NCFET on future processor design

- What is the frequency increase due to NCFET under the same voltage constraint?
- What is the frequency increase under the same (i.e., baseline) power density constraint?
- What is the minimum operating voltage along with the achieved power reduction under the same (i.e., baseline) performance (i.e., frequency) constraint?

H. Amrouch, G. Pahwa, A. D. Gaidhane, J. Henkel, and Y. S. Chauhan, "Negative Capacitance Transistor to Address the Fundamental Limitations in Technology Scaling: Processor Performance", IEEE Access, 2018.

NC-FinFET RF Performance

- Baseline Technology: 10 nm node RF FinFET
- RF Parameters extraction using BSIM-CMG model
- BSIM CMG coupled with L-K for NC-FinFET analysis

R. Singh, K. Aditya, S. S. Parihar, Y. S. Chauhan, R. Vega, T. B. Hook, and A. Dixit, "Evaluation of 10nm Bulk FinFET RF Performance - Conventional vs. NC-FinFET", IEEE Electron Device Letters, Aug. 2018.

NC-FinFET RF Performance

- Current gain ($\propto g_m/c_{gg}$) is almost independent of t_{fe} as both the g_m and C_{gg} increase with t_{fe} almost at a constant rate.
- Cut-off frequency (f_T) remains identical for both the Baseline and NC-FinFET.
- Temperature rise and Power consumption due to self-heating increase with t_{fe} as I_d increases. Reduce V_{dd} to achieve energy efficient performance.

NC-FinFET RF Performance

- g_{ds} and self heating ($\Delta G_{SHE} \propto g_{ds}(f) - g_{ds}(dc)$) both increase with t_{fe} due to increased capacitance matching between C_{fe} and C_{int} .
- Voltage gain ($A_V = g_m/g_{ds} = C_{fe}/C_{GD}$) decreases with t_{fe} due to decrease in C_{fe} .
- Maximum oscillation frequency (f_{max}) also reduces with t_{fe} which can be compensated by reducing V_{dd} .

$$g_{ds} = \frac{\partial I_{ds}}{\partial V_{ds}} = \frac{\partial I_{ds}}{\partial V_{int}} + \frac{\partial V_{int}}{\partial V_{ds}} = g_{m}^{int} + A_V^D \text{ where } A_V^D = \frac{-C_{GD} D I}{|C_{fe}| - C_{int}}$$

Impact of Process Variations

- Variability in I_{ON} , I_{OFF} , and V_t due to combined impact of variability in L_g , T_{fin} , H_{fin} , EOT, t_{fe} , E_c , and P_t
- I_{ON} : Improvement is non-monotonic with t_{fe}
- I_{OFF} : Decreases monotonically with t_{fe}
- V_t : Decreases monotonically with t_{fe}

Process Variation in Ring Oscillator

- The overall average delay variability in NC-FinFET based RO is lesser compared to the reference RO.
- The improvement is non-monotonic with nominal FE thickness scaling.

11-stage Ring-Oscillator: Variation in τ due to combined variation

Open Questions

- Is NC a static or transient phenomenon?
- Physical explanation of NC effect
- Second order effects
 - Impact of grain boundaries and their sizes
 - Impact of multi-domain effects
 - Impact of traps
 - Impact of FE thickness
 - Reliability, Variability
- Impact of NDR/NDIBL on circuits

Relevant Publications

- G. Pahwa, A. Agarwal and Y. S. Chauhan, "Numerical Investigation of Short-Channel Effects in Negative Capacitance MFIS and MFMS Transistors: Above Threshold Behavior," in *IEEE Transactions on Electron Devices*, 2019.
- A.D. Gaidhane, G. Pahwa and Y.S. Chauhan, "Modeling of Inner Fringing Charges and Short Channel Effects in Negative Capacitance MFIS Transistor", accepted in *Electron Devices Technology and Manufacturing (EDTM)*, 2019.
- G. Pahwa, A. Agarwal and Y. S. Chauhan, "Numerical Investigation of Short-Channel Effects in Negative Capacitance MFIS and MFMS Transistors: Subthreshold Behavior," in *IEEE Transactions on Electron Devices*, Nov. 2018.
- Karishma Qureshi, G. Pahwa and Y.S. Chauhan, "Impact of Linear Intergranular Variation in Remnant Polarization on Negative Capacitance Field Effect Transistor", *ICEE*, 2018.
- A.D. Gaidhane, G. Pahwa and Y.S. Chauhan, "Compact Modeling of Drain Current in Double Gate Negative Capacitance MFIS Transistor", *ICEE*, 2018.
- H. Amrouch, G. Pahwa, A. D. Gaidhane, J. Henkel and Y. S. Chauhan, "Negative Capacitance Transistor to Address the Fundamental Limitations in Technology Scaling: Processor Performance," *IEEE Access*, Sep. 2018.
- A.D. Gaidhane, G. Pahwa, A. Verma, Y. S. Chauhan, "Compact Modeling of Drain Current, Charges, and Capacitances in Long-Channel Gate-All-Around Negative Capacitance MFIS Transistor," *IEEE Transactions on Electron Devices*, May 2018.
- G. Pahwa, T. Dutta, A. Agarwal, and Y. S. Chauhan, "Physical Insights on Negative Capacitance Transistors in Non-Hysteresis and Hysteresis Regimes: MFMS vs MFIS Structures", *IEEE Transactions on Electron Devices*, Mar. 2018.
- T. Dutta, G. Pahwa, A. Agarwal, and Y. S. Chauhan, "Impact of Process Variations on Negative Capacitance FinFET Devices and Circuits", *IEEE Electron Device Letters*, Jan. 2018.

07/09/2020

Yogesh Chauhan, IITK

139

Relevant Publications

- T. Dutta, G. Pahwa, A. Agarwal, and Y. S. Chauhan, "Performance Evaluation of 7 nm Node Negative Capacitance FinFET based SRAM", *IEEE Electron Device Letters*, Aug. 2017.
- G. Pahwa, T. Dutta, A. Agarwal, and Y. S. Chauhan, "Compact Model for Ferroelectric Negative Capacitance Transistor with MFIS Structure", *IEEE Transactions on Electron Devices*, Mar. 2017.
- G. Pahwa, T. Dutta, A. Agarwal, S. Khandelwal, S. Salahuddin, C. Hu, and Y. S. Chauhan, "Analysis and Compact Modeling of Negative Capacitance Transistor with High ON-Current and Negative Output Differential Resistance - Part I, Model description", *IEEE Transactions on Electron Devices*, Dec. 2016.
- G. Pahwa, T. Dutta, A. Agarwal, S. Khandelwal, S. Salahuddin, C. Hu, and Y. S. Chauhan, "Analysis and Compact Modeling of Negative Capacitance Transistor with High ON-Current and Negative Output Differential Resistance - Part II, Model validation", *IEEE Transactions on Electron Devices*, Dec. 2016.
- G. Pahwa, T. Dutta, A. Agarwal, and Y. S. Chauhan, "Energy-Delay Tradeoffs in Negative Capacitance FinFET based CMOS Circuits", *IEEE ICEE*, Dec. 2016. (*Best Paper Award*)
- G. Pahwa, T. Dutta, A. Agarwal, and Y. S. Chauhan, "Designing Energy Efficient and Hysteresis Free Negative Capacitance FinFET with Negative DIBL and 3.5X ION using Compact Modeling Approach", *IEEE ESSDERC*, Switzerland, Sept. 2016. (*Invited*)
- G. Pahwa, A. Agarwal, and Y. S. Chauhan, "Compact Modeling of Negative Capacitance Transistor with Experimental Validation", *IWPSD*, Dec. 2015.

07/09/2020

Yogesh Chauhan, IITK

140

Summary

- Industry standard model development @ IITK
- All models are implemented in the **Verilog - A** code
 - Tested on commercial **simulators**
 - Validated with real device data
- Working with major semiconductor and EDA companies

07/09/2020

Yogesh Chauhan, IITK

141